

# Axial resistance of piles during driving in chalk

## Résistance axiale des pieux lors du battage dans la craie

T. Liu\*

*University of Bristol, Bristol, UK*

R.M. Buckley

*University of Glasgow, Glasgow, UK*

B.W. Byrne

*University of Oxford, Oxford, UK*

S. Kontoe

*University of Patras, Patras, Greece; Imperial College London, London, UK*

R.J. Jardine, K. Vinck

*Imperial College London, London, UK*

R.A. McAdam

*Ørsted Power Ltd, London, UK*

\*[tingfa.liu@bristol.ac.uk](mailto:tingfa.liu@bristol.ac.uk)

**ABSTRACT:** The driveability and axial capacity of driven piles depend critically on their geometry, end conditions and the degree of drainage they experience during driving. This paper summarises the installation characteristics of 41 impact-driven piles driven for the ALPACA joint industry project (JIP). The installed piles covered open- and closed-ended steel tubular, sheet and reinforced square concrete piles with a wide range of diameters (from 139 mm to 1.8 m), wall thickness ratios (14 to 72), and embedment length-to-diameter ratios (6 to 40). Analyses that applied parameters interpreted from parallel piezocone penetration and dissipation tests indicated that pore-pressures of several MPa developed beneath large open-ended piles during rapid driving and led to surprisingly low shaft resistances. However, the slower driving of the closed-ended concrete and sheet piles permitted far higher degrees of dissipation and led to far greater shaft resistances. Signal matching analyses demonstrate how the End of Driving (EoD) shaft resistances were affected strongly by de-structuring of the chalk and the relative depth of the pile tip. The EoD shaft resistances corresponded closely with predictions made applying the short-term Chalk ICP-18 Soil Resistance to Driving (SRD) formulae. An updated base resistance formula was proposed that correlates with pile wall thickness ratio.

**RÉSUMÉ:** La capacité de battage et la capacité axiale des pieux battus dépendent essentiellement de leur géométrie, de conditions d'extrémité et du degré de drainage pendant le battage. Cet article résume les caractéristiques d'installation de 41 pieux battus par impact pour le projet industriel commun ALPACA, incluant des pieux tubulaires en acier à extrémités ouvertes et fermées, des tôles et des pieux carrés en béton armé, avec des diamètres (139 mm à 1,8 m), des rapports d'épaisseur de paroi (14 à 72) et de longueur d'ancrage par diamètre (6 à 40). Des analyses utilisant des paramètres interprétés à partir d'essais de pénétration et de dissipation de piézocônes parallèles ont indiqué que des pressions interstitielles de plusieurs MPa se développaient sous de grands pieux à extrémité ouverte lors d'un battage rapide et conduisaient à des résistances d'arbre étonnamment faibles. Cependant, l'enfoncement plus lent des palplanches et du béton à extrémité fermée a permis des degrés de dissipation beaucoup plus élevés et a conduit à des résistances d'arbre bien plus grandes. Les analyses d'appariement des signaux démontrent comment les résistances de l'arbre en fin de battage (EoD) ont été fortement affectées par la déstructuration de la craie et la profondeur relative de la pointe du pieu. Les résistances des arbres EoD correspondaient étroitement aux prédictions faites en appliquant les formules à court terme de Chalk ICP-18 Soil Resistance to Driving (SRD). Une formule de résistance de base mise à jour a été proposée, en corrélation avec le rapport d'épaisseur de paroi du pieu.

**Keywords:** Chalk; impact driving; chalk resistance to driving (CRD); axial capacity; signal matching.

## 1 INTRODUCTION

Chalk is a high-porosity, calcareous, variable soft biomicrite found in large areas of North West Europe and other regions worldwide (Mortimore, 2012).

Large open-ended driven piles are employed to support a wide range of onshore and offshore infrastructure at chalk sites. However, their driveability has proven challenging to predict. Refusal

has been reported on driving through high density chalk while strikingly low average shaft resistances (sometimes well below 20 kPa) can be developed on driving through low-to-medium density chalk, attributing to uncontrolled self-penetration (or 'runs') to far greater-than-expected depths (Carotenuto et al., 2018). Buckley et al. (2021) proposed a short-term 'Chalk ICP-18' Resistance to Driving (CRD) approach based on back-analyses of onshore and offshore

driving records of open-ended piles with respective length-to-diameter and wall thickness ratios of  $5 \leq L/D \leq 40$  and  $17 \leq D/t_w \leq 67$  driven in structured low-to-medium density chalks with corrected cone resistances ( $q_t$ ) broadly between 10 and 20 MPa. They also suggested that the annular base resistances ( $q_b$ ) developed during driving amount to around  $0.6q_t$ .

Jardine et al. (2023a, b) report how the significant uncertainties and challenges involved in designing driven pile foundations to sustain axial and lateral, monotonic and cyclic loading in chalk were addressed in the major ALPACA (Axial-lateral pile analysis for chalk applying multiscale field and laboratory testing) and ALPACA Plus joint industry research projects. Forty-one instrumented piles were driven at the well-characterised St Nicholas at Wade low-to-medium density chalk site in Kent, UK (Vinck et al., 2023) and comprehensive testing undertaken that led to new design guidelines for all the above loading cases.

This paper summarises the key phenomena observed during driving with dynamic instruments mounted on all piles and the findings obtained from rigorously conducted stress wave record numerical matching analyses. The performance of the Chalk ICP-18 CRD predictive approach was checked against the extended dataset, and the base driving resistance formula updated to account for wall thickness ratio.

## 2 PILE INSTALLATION OBSERVATIONS

Table 1 summarises the ALPACA and ALPACA Plus ranges for pile diameter  $D$  (139 mm – 1.8 m),

slenderness ratio ( $L_p/D$ ) (6 – 40), wall thickness ratio ( $D/t_w$ ) (14 – 72), tip conditions, geometry and shaft materials. Also listed are the hammer masses, non-dimensional average velocities  $V$  ( $= vD/c_h$ ), upper bound full drainage elapsed times and end-of-driving average shaft resistances ( $\tau_{avg}^{EoD}$ ) back analysed from stress-wave matches. All piles were monitored with above-ground pile driving analyser (PDA) strain gauges and accelerometers; 16 were instrumented with paired Fibre Bragg Grating optical strain gauge strings embedded along their shafts (Buckley et al., 2020).

All the open-ended piles drove in a fully coring manner with internal chalk columns that extruded and rose well above ground level at the end of driving, confirming relatively little outward volume displacement into the stiff surrounding chalk mass. Figure 1 shows how the volume displaced above ground compared to that of the embedded steel,  $V_{pag}/V_{steel}$ , fell systematically with  $L_p/D$ ; open-pile cores rarely rise above ground level in sands and clays.

Driving the open-tubular LD and SD piles to target depths with the employed hammers required 9 to 55 blows per 250 mm and total driving times of 2 to 14 minutes. Relatively hard driving was required for (i) the 200 mm square concrete piles, with up to 308 blows/250 mm over up to 81 minutes and (ii) the sheet piles with up to 100 blows/250 mm and  $\approx 20$ -minute driving times, leading to relatively low  $V$  values. These piles' slow driving is likely to have led to greater degrees of drainage that attributed to higher  $\tau_{avg}^{EoD}$  (83.3 and 37.1 kPa respectively) average shaft resistances than the 24.8 kPa of open-ended piles.

Table 1. ALPACA and ALPACA Plus driven pile installation: pile geometries, conditions, hammer details, ranges of normalised velocity  $V$ , upper bound full drainage elapsed times and end-of-driving (EoD) average shaft resistances ( $\tau_{avg}^{EoD}$ ).

| Pile numbers, codes and material                      | $D$ (mm) | $t_w$ (mm) | $R^*$ (m) | $L_p$ (m) | $L_p/D$ | Hammer (ram mass)       | Norm. $V$ ( $= vD/c_h$ ) | Upper bound $t_{95}$ (min) | $\tau_{avg}^{EoD}$ (kPa) |
|---|----------|------------|-----------|-----------|---------|-------------------------|--------------------------|----------------------------|--------------------------|
| 12 'LD' open-ended steel                              | 508      | 20.6       | 0.100     | 10.16     | 20      | Juntann SHK-4 (4 ton)   | 1.54 – 2.09              | 27.9                       | 15.6 – 28.0              |
| 2 'LD' open-ended steel                               | 508      | 20.6       | 0.100     | 3.05      | 6       | HHK-5A (5 ton) for LD14 | 0.79 – 1.67              | 27.9                       | 19.8 – 31.3              |
| 16 'SD' open-ended steel, including 2 stainless steel | 139      | 8.0 – 10.3 | 0.035     | 4.9 – 5.5 | 38 – 40 |                         | 0.52 – 1.50              | 3.4                        | 18.1 – 27.4              |
| 2 'SD' closed-ended steel                             | 139      | 9.4 – 9.7  | 0.070     | 5.4 – 5.5 | 39 – 40 | Delmag (1.4 ton)        | 0.36 – 1.20              | 13.4                       | 19.7                     |
| 2 concrete square                                     | 226      | NA         | 0.113     | 4.9 – 5.4 | 22 – 24 |                         | 0.10 – 0.16              | 35.5                       | 83.3                     |
| 2 SM-J steel sheet piles                              | 290      | 11 – 12.2  | 0.057     | 5.4       | 18.6    |                         | 0.24                     | 9.0                        | 37.1                     |
| TP1 open-ended steel                                  | 1800     | 25         | 0.211     | 18        | 10      | BSP CG240 (16 ton)      | 2.74                     | 123.4                      | 26.2                     |
| TP2 and R1 open-ended steel                           | 1220     | 24.6       | 0.171     | 7.3       | 6       | BSP CX110 (9 ton)       | 1.64 – 2.48              | 81.8                       | 22.1 – 31.3              |
| R2 open-ended steel                                   | 1220     | 24.6       |           | 18        | 14.8    |                         |                          |                            | 24.2                     |
| TP3 open-ended steel                                  | 508      | 12.5       | 0.079     | 18        | 35.4    |                         | 0.50                     | 17.2                       | 26.9                     |

Notes:  $D$  listed for concrete and sheet piles based on equivalent area;  $t_w$ : pile wall thickness;  $R^*$ : equivalent radius for open-ended piles ( $= (R^2 - R_i^2)^{0.5}$ );  $R$  and  $R_i$ : outer and inner radius, respectively;  $c_h$ : coefficient of horizontal consolidation.

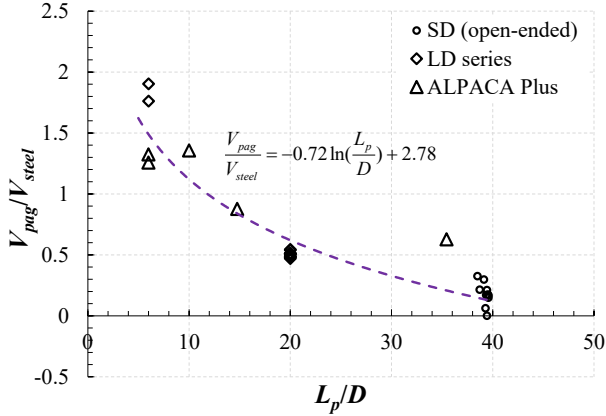


Figure 1. Variation of the ratio between the above-ground chalk plug volume ( $V_{pag}$ ) and embedded steel volume ( $V_{steel}$ ) against  $L_p/D$ .

### 3 DRIVING RESISTANCE PREDICTIONS

#### 3.1 ALPACA shaft and base CRD formulae

Buckley et al. (2020) show that internal shaft resistances are likely to be far lower than apply externally to piles driven in chalk. The overall shear resistances are therefore considered in Chalk ICP-18 as the sum of the external and internal shaft stresses and treated as applying only on the external pile shaft. The overall shear resistances available at any level on the shaft,  $\tau_{rzi}$ , are determined through Equation (1), in which  $\sigma_{ri}'$  denotes radial effective stress during installation and  $\delta_{ult}'$  interface shear resistance angle determined from Bishop ring shear interface tests and typically taken as  $32^\circ$  (Vinck, 2021).

$$\tau_{rzi} = \sigma_{ri}' \tan \delta_{ult}' \quad (1)$$

The local radial effective stress ( $\sigma_{ri}'$ ) and base bearing pressure ( $q_b$ ) are defined as functions of relative pile tip depth ( $h$ ), corrected cone resistance ( $q_t$ ), equivalent radius ( $R^*$ ) and  $D/t_w$ :

$$\sigma_{ri}' = 0.031 q_t \left( \frac{h}{R^*} \right)^{-0.481} \left( \frac{D}{t_w} \right)^{0.145} \quad (2)$$

$(h/R^* \geq 6)$

$$R^* = (R^2 - R_i^2)^{0.5} \quad (3)$$

$$q_b = q_t (D/t_w)^{-0.175} \quad (4)$$

#### 3.2 Performance of the method in predicting field behaviour

The performance of the Chalk ICP-18 shaft CRD method was assessed systematically against the dynamic stress-wave matches of the ALPACA and ALPACA Plus piles' instrumented driving records, as well as independent cases collated and analysed by Vinck (2021).

Overall comparison of the total EoD shaft load between the predictions for shaft resistance  $Q_s$  integrated from the above expressions and the signal-matching outcomes, indicated a fortuitously unbiased mean calculated-to-measured ( $Q_c/Q_m$ ) ratio of 1.00 and a coefficient of variation ( $CoV$ ) of 0.38 for the open-ended piles listed in Table 1. The latter  $CoV$ , which should be recognised when developing upper and lower bound CRD profiles for hammer selection and pile fatigue analyses, reflects natural variabilities of chalk conditions and driving operations as well as uncertainties inherent in stress wave matching.

Further testing of the approach by Vinck et al. (2023) at the Sauchay medium density chalk test site near Dieppe in France also showed good agreement with mean  $Q_c/Q_m$  of 0.99 and  $CoV$  of 0.19.

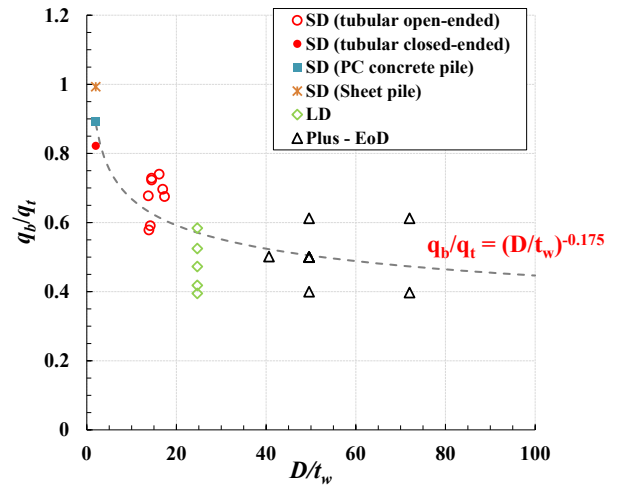


Figure 2. Normalised bearing pressure ( $q_b/q_t$ ) against piles'  $D/t_w$  at end-of-driving (Note:  $q_b$  evaluated over closed-ended piles' full areas and open-ended piles' steel annuli;  $D/t_w$  taken as 2 for closed-ended piles).

However, Jardine et al. (2023b) and Vinck et al. (2023) proposed from their analyses that the base driving resistance formula required updating. Figure 2 plots the signal-matched End-of-Driving base resistance ( $q_b$ ) values normalised by  $q_t$  against  $D/t_w$ , showing a declining trend that can be expressed by power-law Equation (4). This updated method leads to

a better and more conservative fit to the data than the Chalk ICP-18's tentatively suggested  $q_b/q_t \approx 0.6$ .

Two examples from the signal matching analyses are shown in Figure 3. The shaft resistance profiles derived from signal matching back analyses are compared with predictions from Equations (1)-(3) for both relatively long ( $L_p/D = 20$ ) and short ( $L_p/D = 6$ ) open steel, 508mm outside diameter piles (LD5 and 13 respectively). Two  $q_t$  profiles are also shown, as established in CPT soundings made close to both piles.

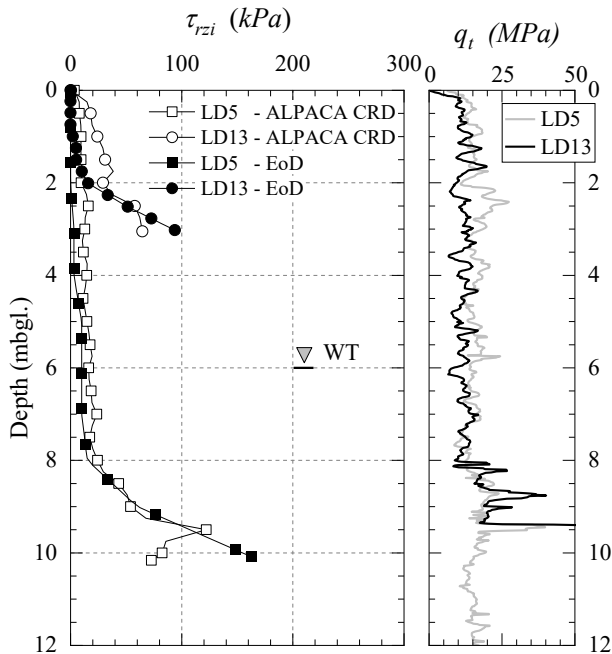


Figure 3. Profiles of CPT resistance and shaft friction from EoD PDA analysis against CRD prediction for two LD piles ( $D = 508 \text{ mm}$ ,  $D/t_w = 25$ ).

#### 4 CONCLUSIONS

- (1) Predicting pile's driveability in chalk is crucial to many onshore and offshore projects.
- (2) Comprehensive research was undertaken in the ALPACA and ALPACA Plus campaigns on 41 instrumented piles to (i) improve fundamental understanding of driving resistances and (ii) calibrate new predictive approaches. Axial driving resistances were found to depend critically on pile geometry, end conditions, CPT resistance and any drainage during installation.
- (3) Closed-ended sheet and concrete piles experienced relatively hard driving that permitted higher degrees of drainage and higher driving resistances.
- (4) Rigorous stress wave analyses confirmed that the Chalk ICP-18 resistance to driving (CRD) method led to unbiased shaft predictions for the St Nicholas at Wade (SNW) piles and generally good matches

in other independent cases. The test analysis also allowed an improvement of the method's formulation for base resistance to driving.

#### ACKNOWLEDGEMENT

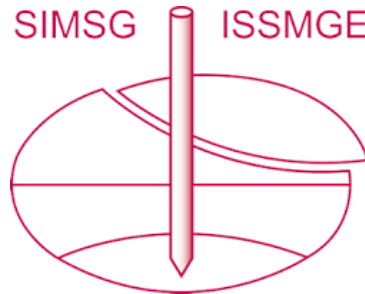
The Authors gratefully acknowledge support from UK grants from EPSRC (EP/P033091/1), Royal Society (NA160438) and Supergen ORE Hub 2018 (EPSRC EP/S000747/1). Byrne is supported by the Royal Academy of Engineering under the Research Chairs and Senior Research Fellowships scheme, while Vinck was supported by EPSRC Grant EP/L016826/1, DEMA and Imperial College. Financial and technical support by the following project partners is also acknowledged gratefully: Atkins, Cathies, Equinor, Fugro, GCG, LEMS, Ørsted, Parkwind, RWE, Siemens-Gamesa, Scottish Power Renewables and Vattenfall. The Authors also wish to acknowledge Socotec UK Ltd as the principal contractor for the ALPACA and ALPACA Plus field testing campaigns.

#### REFERENCES

- Buckley, R.M., McAdam, R.A., Byrne, B.W., Doherty, J.P., Jardine, R.J., Kontoe, S., and Randolph, M.F. (2020). Optimisation of impact pile driving using optical fibre Bragg grating measurements. *Journal of Geotechnical and Geoenvironmental Engineering*, 146(9). [https://doi.org/10.1061/\(ASCE\)GT.1943-5606.0002293](https://doi.org/10.1061/(ASCE)GT.1943-5606.0002293).
- Buckley, R.M., Kontoe, S., Jardine R.J., Barbosa, P. and Schroeder, F.C. (2021). Pile driveability in low- to medium-density chalk. *Canadian Geotechnical Journal*, 58(5): 650-665. <https://doi.org/10.1139/cgj-2019-0703>.
- Carotenuto, P., Meyer, V., Strøm, P.J., Cabarkapa, Z., St. John, H. and Jardine, R.J. (2018). Installation and axial capacity of the Sheringham Shoal offshore wind farm monopiles—a case history. Proceedings of the Engineering in Chalk Conference (Lawrence J.A., Preene M., Lawrence U.L. and Buckley R.M.(eds)), Institution of Civil Engineers (ICE) Publishing, London <https://doi.org/10.1680/eiccf.64072.117>.
- Jardine, R.J., Buckley, R.M., Liu, T., Byrne, B.W., Kontoe, S., McAdam, R.A., Schranz, F. and Vinck, K. (2023a). The ALPACA and ALPACA Plus Joint Industry studies of driven pile behaviour in low-to-medium density chalk. Proceedings of 9<sup>th</sup> International Offshore Site Investigation and Geotechnics Conference, London. The Society for Underwater Technology.
- Jardine, R.J., Buckley, R.M., Liu, T., Andolfsson, T., Byrne, B.W., Kontoe, S., McAdam, R.A., Schranz, F. and Vinck, K. (2023b). The axial behaviour of piles driven in chalk. *Géotechnique*, Ahead of Print. <https://doi.org/10.1680/jgeot.22.00041>.
- Lord, J.A., Clayton, C.R.L. and Mortimore, R.N. (2002). Engineering in chalk, CIRIA, C574.

- Vinck, K. (2021). Advanced geotechnical characterisation to support driven pile design at chalk sites. PhD thesis, Imperial College London.
- Vinck, K., Liu, T., Jardine R.J., Kontoe, S., Ahmadi-Naghadeh, R., Buckley, R.M., Byrne, B.W., Lawrance, J.A., McAdam, R.A. and Schranz, F. (2022). Advanced in-situ and laboratory characterisation of the ALPACA chalk research site. *Géotechnique*, Ahead of Print. <https://doi.org/10.1680/jgeot.21.00197>.
- Vinck, K., Liu, T., Mawet, J., Kontoe, S. and Jardine, R.J. (2023). Field tests on large scale instrumented piles driven in chalk: results and interpretation. *Canadian Geotechnical Journal*, 60(10), 1475-1490: <https://doi.org/10.1139/cgj-2022-0441>.

# INTERNATIONAL SOCIETY FOR SOIL MECHANICS AND GEOTECHNICAL ENGINEERING



*This paper was downloaded from the Online Library of the International Society for Soil Mechanics and Geotechnical Engineering (ISSMGE). The library is available here:*

<https://www.issmge.org/publications/online-library>

*This is an open-access database that archives thousands of papers published under the Auspices of the ISSMGE and maintained by the Innovation and Development Committee of ISSMGE.*

*The paper was published in the proceedings of the 18th European Conference on Soil Mechanics and Geotechnical Engineering and was edited by Nuno Guerra. The conference was held from August 26<sup>th</sup> to August 30<sup>th</sup> 2024 in Lisbon, Portugal.*